Published in final edited form as:
J Neurosci. 2008 May 7; 28(19): 4878–4887. doi:10.1523/JNEUROSCI.0828-08.2008.

Dicer inactivation leads to progressive functional and structural degeneration of the mouse retina

Devid Damiani[1], **John J Alexander**[2], **Jason R O'Rourke**[3], **Mike McManus**[4], **Ashutosh P Jadhav**[5], **Constance L Cepko**[5], **William W Hauswirth**[2], **Brian D Harfe**[3], and **Enrica Strettoi**[1]

[1]Neuroscience Institute, Italian National Research Council, Pisa, Italy

[2]Department of Ophthalmology, University of Florida College of Medicine, Gainesville, FL, USA

[3]Department of Molecular Genetics and Microbiology, University of Florida College of Medicine, Gainesville, FL, USA

[4]Department of Microbiology and Immunology, University of California, San Francisco, CA, USA

[5]Department of Genetics, Harvard Medical School, Boston, USA

Abstract

MicroRNAs (miRNAs) are small, highly conserved molecules that have been shown to regulate the expression of genes by binding to specific target mRNAs. Dicer, an RNase III endonuclease, is essential for the production and function of mature miRNAs and removal of *Dicer* has been shown to disrupt many developmental processes. In this report, *Dicer* was removed specifically from the retina using a floxed *Dicer* conditional allele and the retinal *Chx10Cre* transgene. Retinal *Dicer* knockout mice displayed a reproducible inability to respond to light. In addition, morphological defects were observed with the formation of photoreceptor rosettes at P16 which progressed to more general cellular disorganization and widespread degeneration of retinal cell types as the animals aged. This was accompanied by concomitant decrease in both scotopic and photopic ERG responses. Interestingly, removing a single allele of *Dicer* resulted in ERG deficits throughout life but not to morphological abnormalities. Northern blot analysis of *Dicer* depleted retinas showed a decrease in several microRNAs. The observation that progressive retinal degeneration occurred upon removal of *Dicer* raises the possibility that miRNAs are involved in retinal neurodegenerative disorders.

Keywords

Dicer; miRNA; photoreceptors; bipolar cells; rosettes; horizontal cells; retinal degeneration; ERG

Introduction

MicroRNAs (miRNAs) encode small 21-nt single-stranded RNAs that recently have been shown to regulate gene expression in a large number of diverse organisms and tissues (Cao et al., 2006). In vertebrates, miRNAs most often function as negative regulators of gene expression by base pairing with the 3'-untranslated region (3'-UTR) of target mRNAs while part of RNA-induced silencing complexes (RISCs). More than 400 miRNAs have been

Corresponding authors: **Enrica Strettoi**, Istituto di Neuroscienze CNR, Via G. Moruzzi 1, 56100 Pisa Italy, office: +39 050 315 3213, Fax: +39 050 315 3212, enrica.strettoi@in.cnr.it **Brian D. Harfe**, University of Florida, College of Medicine, Gainesville, FL 32608, USA, Phone office: 352-273-8078, Fax: 352-273-8284, bharfe@mgm.ufl.edu.
Senior Editor: Dr. Moses Chao

identified in both mice and humans, and each miRNA has the potential to regulate hundreds of target genes (Ambros and Cen, 2007; Lagos-Quintana et al., 2002). It has been proposed that more than one third of all human genes may be regulated by miRNAs (Lewis et al., 2005). Approximately 70% of experimentally detectable miRNAs are expressed in the brain, and among those upregulated in a tissue specific expression pattern in the embryo, half are brain-specific/enriched (Cao et al., 2006; Babak et al. 2004, Barad et al. 2004, Miska et al. 2004, Sempere et al. 2004, Thomson et al. 2004).

miRNAs are processed by Dicer, a double-stranded RNA-specific endonuclease, from a non-functional ~70-nt precursor RNA to a functional ~21-nt molecule (Ambros et al. 2003). Dicer null mice have been reported to die at embryonic day 7.5 (Bernstein et al. 2003) rendering it impossible to study the role Dicer may play in later stages of development or in adult tissues. To bypass the early lethality associated with the removal of Dicer in all tissues, we recently created a floxed conditional *Dicer* allele (Harfe et al., 2005). Using this allele in conjunction with tissue-specific *cre* alleles, we and others have inactivated Dicer in a number of discrete tissues during both embryonic and postnatal life (i.e. Harfe et al., 2005; Harris et al., 2006; O'Rourke et al., 2007). Since Dicer is required for the processing of miRNAs, removal of Dicer results in a significant decrease in functional miRNAs.

In spite of their abundance in the brain, detailed functional studies of miRNAs in the nervous system have not been provided until very recently (Cuellar et al., 2008; Davis et al., 2008). In this report we used the *Dicer* conditional mouse in combination with a retinal *Chx10Cre* transgenic line (Rowan and Cepko, 2004) to assess the role miRNA-mediated regulation of gene expression plays in the developing and adult murine retina.

Our data demonstrate that inactivation of Dicer in the retina results in progressive and widespread structural and functional abnormalities, culminating in loss of photoreceptor mediated responses to light and extensive retinal degeneration. This is the first study of miRNA inactivation within the mammalian eye and suggests that miRNAs play an essential role in neural tissue homeostasis. The degenerative phenotype reported here raises the possibility that miRNAs may be involved in some retinal diseases, and perhaps more generally, in neurodegenerative disorders as suggested by recent results obtained in mice with a conditional knockout of Dicer in Purkinje cells (Schaefer et al., 2007).

Methods

Generation and genotyping of CKO mice

Construction and genotyping of the *Dicer* and *Chx10Cre* alleles has been described previously (Harfe et al., 2005; Rowan and Cepko, 2004). To create mice in which Dicer was inactivated in the retina, males containing the *Chx10Cre* transgene were crossed to females homozygous for the *Dicer* conditional allele. This cross generated animals in which one *Dicer* allele was removed in the retina ("heterozygous animals"). Heterozygous mice were then used to create $Dicer^{flox}/Dicer^{flox}$;*Chx10Cre* animals (referred to as "CKO"). CKO animals were viable and did not contain any obvious systemic phenotypic defects. $Dicer^{flox}/Dicer^{flox}$ mice were used as wild type controls in all experiments. All animals used in our analysis were outcrossed at least three times onto a C57Bl/6 genetic background.

$Dicer^{flox}/Dicer^{flox}$;*Chx10Cre* animals were crossed to R26R mice (Soriano, 1999) to visualize cells that had undergone a recombination event.

Electrophysiology

Mice were dark adapted overnight in a Faraday shielded room and all subsequent procedures were carried out under dim red light (>650 nm). The corneas of the mice were given drops

of 1% atropine, 2.5% phenylephrine and 0.5% proparacaine (Akorn, Buffalo Grove, IL) for mydriasis and topical corneal anesthesia. The mice were then anesthetized by intraperitoneal injection (6 µL per gram) of a sterile mixture of 100 mg/mL ketamine, 20 mg/mL xylazine, and normal saline at a 1:1:5 ratio, respectively. When the mice were fully sedated, they were placed onto a heated ERG platform in ventral recumbency. Balanced salt solution (Alcon, Ft. Worth, Tx) and Gonak (Akorn, Buffalo Grove, IL) were used to lubricate the cornea prior to electrode placement. Custom platinum loop electrodes were positioned on the cornea using a 3-axis micro-positioning system (Narishige, Japan). Grass platinum subdermal needle electrodes (Grass, West Warwick, RI) were utilized for ground and reference. All ERG's were performed using a Multiliner Vision (Jaeger/Toennies, Hochberg, Germany) system equipped with a Ganzfeld-stimulator (Jaeger/Toennies, Hochberg, Germany). The Multiliner Vision apparatus complies with and exceeds the relevant International Society for Clinical Electrophysiology of Vision standards. Unless otherwise indicated, all mice were tested for dark-adapted ERG responses followed by light-adapted ERG responses. White light from a xenon source was used as the stimulus. For the scotopic (dark-adapted) ERG series, mice were exposed to a series of 10 flashes at 0.1 cd•s/m^2. For the photopic (light-adapted) ERG series, mice were exposed to background light at 100 cd/m^2 for 1 minute and ERG recordings were done in the presence of a constant 100 cd/m^2 background light. Mice were then exposed to a series of 50 flashes at 10 cd•s/m^2. Right and left eyes were tested simultaneously and the data recorded. Analysis of the ERG waveforms for a-and b-wave maxima was carried out using the Multiliner Vision software. Further analysis was performed using Sigma Plot software. When calculating significance a Student's t-test was used.

Northern Blot

Retinas from 1 month (n=3, mutant; n=6, wt), 3 months (n=3, mutant; n=2 wt) and 24 months (n=2 mutant; n=3 heterozygous; n=2 wt) animals were pooled. RNA was isolated from fresh homogenized pooled retinas with TRI Reagent (Sigma). Approximately 12 µg of total RNA for the 1 and 3 month time points and ~8 µg of total RNA from 24 month animals was resolved on 10% urea/polyacrylamide gels and electroblotted to Hybond N^+ membranes (Amersham) at 200 mA for 3 h. Blots were crosslinked using a Stratalinker (Stratagen) and prehybridized for at least 1 h at 37°C in ULTRAhyb™-Oligo (Ambion) hybridization buffer before overnight incubation at 37°C in hybridization buffer containing [^{32}P]-end-labeled probe. Probes were generated by end-labeling 20 pmols of DNA oligonucleotide (Invitrogen) complementary to a specific miRNA or U6 with T4 polynucleotide kinase (New England Biolabs) and 250 µCi [γ-^{32}P] ATP (Perkin Elmer) followed by purification with MicroSpin™ G-25 columns (Amersham). Blots were washed (2X SSC, 0.1% SDS) at 37°C for 30 min followed by two 30 min room temperature washes. Blots were exposed to Kodak BioMax film and quantification was determined by densitometry of autoradiographs using ImageQuant TL v2003.02 software. For subsequent probing, blots were stripped by incubating twice in boiling 1% SDS for 15 minutes each and exposed to film to confirm that probes were removed.

In situ hybridization

Whole mouse eyes were fixed overnight in 4% PFA/PBS, infiltrated with 30% sucrose, frozen and sectioned as described below. A 260-nt riboprobe (Harris et al., 2006), specific to the floxed *Dicer* exon was used to assess Dicer distribution. After a brief wash in PBS, retinal sections were treated 2×10 min with RIPA buffer, post-fixed 15 min in 4% PFA /PBS and acetylated with 0,25% acetic anhydride in triethanolamine 0,1 M. Slides were then pre-hybridized for 2 hrs in a solution of 50% formamide, 5× SSC, 5× Denhart's, 500 µg/ml salmon sperm DNA and 250 µg/ml yeast RNA. Slides were hybridized for 12 hrs at 48 °C, with 100–300 ng of digoxigenin labeled probe per slide in a plastic chamber humidified with

50% formamide in 5× SSC. Post-hybridization washes were made with 50% formamide, 0,1% Tween-20 in 2× SSC, for 2 hrs. Sections was then re-equilibrated in 0.1 % Tween-20 in 0.1M maleic acid buffer (MABT), blocked for 1–2 hours in 10 % sheep serum in MABT and incubated for 12 hrs at 4°C with anti-digoxigenin-AP (1/2000 in blocking buffer; Roche). After MABT washing, the pH of the specimens was adjusted with 100 mM Tris pH 9,5, 50 mM $MgCl_2$, 100 mM NaCl. Finally, retinal sections were reacted for 1–2 hrs with NBT-BCIP solution (Sigma), washed in PBS, dehydrated in ethanol, mounted in DPX and acquired with an Zeiss Axioplan microscope, equipped with an AxioCam HRC color camera and dedicated AxioVision software.

BrdU administration

Three intraperitoneal (IP) injections of 50 mg/Kg BrdU were performed at 3 hr intervals in P35 mice (n=5). Mice were then sacrificed 3 hrs after the final injection, their eyes prepared as described above and BrdU detected by immunocytochemistry on frozen retinal sections following the procedure of Close et al., 2005.

Immunocytochemistry (ICCH) and Electron Microscopy (EM)

The eyes of mice aged postnatal (P) 2, 16, 30, 45 days and 3, 4, 5, and 7 months were harvested, quickly enucleated and immersion-fixed for 1 hr in 4% paraformaldehyde in 0.1 M phosphate buffer (0.1M PB). The eyes were then rinsed in buffer, infiltrated overnight in 30% sucrose in 0.1M PB, embedded in OCT/Tissue Tek (Sakura) and frozen on a cryostat stage at −25/−30°C. Eyes were sectioned vertically in 12–16 μm serial sections with a Leica cryostat. Sections were collected on Superfrost Plus slides and air dried for 5 min to 2 hours. Slides were rinsed for 10 min with 0.01M PBS and blocked for 2 hours in a solution containing 5% bovine serum albumin (BSA) and 0.3% Triton-X100 in PBS. Primary antibodies were diluted in 1% BSA, 0.1% Triton X100 in PBS. Slides were incubated in primary antibodies for 12–18 hours at 4°C. Primary antibodies were rinsed off by 2×10 min incubation in PBS at RT. Sections were then incubated for 2–4 hrs in solutions containing appropriate secondary antibodies, diluted 1:400, conjugated with Oregon Green 488, Alexa Fluor 568, Alexa Fluor 647 (Invitrogen) or Cy-3 (Sigma). Sections were then rinsed in PBS and, if appropriate, counterstained with the fluorescent nuclear dyes BOBO-1 or TOTO-3 (Invitrogen).

Primary antibodies and dilutions were as follows: mouse anti-rhodopsin (1:2,500; Sigma); rabbit anti-recoverin (1:2,000; Chemicon); mouse and rabbit anti-protein kinase C-α (PKC-α; 1:1,000; clone MC5, Sigma; sc-208, Santa Cruz Biotechnology); mouse and rabbit anti-calbindin D-28k (1:2,000; clone CB955, Sigma; Swant); mouse anti-G0α (1:1,000; MAB 3073, Chemicon); mouse anti-neurofilament 200 kDa (1:100; NF-200; clone N52, Sigma); rabbit anti-mGluR6 (1:2,000; from Dr. S. Nakanishi, Osaka University, Japan); mouse anti-post-synaptic density protein 95 (1:500; PSD95; AbCam); mouse anti-glutamine synthase (GS; 1:2,000; MAB302, Chemicon); rabbit anti-glial fibrillary acidic protein (1:1,000; GFAP, Sigma); goat anti-choline acetyl transferase (1:500; ChAT; Chemicon); mouse anti-Cre recombinase (1:1,000; MAB3120; Chemicon); rabbit anti-Green Fluorescent Protein-Alexa Fluor 488 conjugate (1:1,000; Invitrogen); rabbit anti-phosphohistone H3 (1:400; Upstate); rabbit anti atypical PKC (C20, 1:500, Santa Cruz Biotechnology); rabbit anti zonula occludens-1 (ZO-1; 1: 200, Zymed); rabbit anti laminin (1:400, Sigma); guinea pig anti vesicular glutamate transporter (vGLUT1, 1:500, Chemicon); rabbit anti vesicular GABA transporter (vGAT 1:500, Synaptic System). Rabbit anti S-cone opsin (1:1000, Chemicon) and Alexa Fluor 488-PNA lectins (1:400; Invitrogen) were used to label cone photoreceptors.

Retinal preparations were examined with a Leica TCS-NT confocal microscope equipped with an argon-krypton laser or with a Leica TCS-SL spectral confocal microscope using high numerical aperture oil immersion objectives. Images acquired at a resolution of 1024×1024 were saved as TIFF files and exported on a workstation for offline analysis. Retinas from at least one wild type, one heterozygote and three CKO littermates for each age group (2, 16, 30, 45 days and 3, 4, 5 and 7 months) were used for ICCH and screened with the full panel of antibodies listed above. A total of 57 animals were analyzed for ICCH. Except for P2 and P16 animals, eyes used for morphological analysis were from animals previously used for ERG recordings (see below).

One additional litter composed of 4 mutants and 5 wild type animals aged P2 was used for EM studies of immature retinas. After decapitation, the eyes were removed and immersion-fixed in 2% PAF and 2.5% glutaraldehyde for 12 hrs. After dissections, retinal tissue was postfixed in osmium tetroxide, bloc stained with 1% uranyl acetate, dehydrated in ethanol and embedded in plastic. Semithin sections (1–2 micrometer thick) were stained with Epoxy Tissue stain (EMS) and observed at the light microscope. Ultrathin sections from retinal blocs were counterstained with uranyl acetate and lead citrate and examined with a Jeol 1200 EXII electron microscope. Photographs of retinal neuroblasts and differentiating photoreceptors were taken at 8,000–20,000X.

Results

ERG abnormalities in CKO animals

An analysis of electroretinograms (ERG) recorded from 1, 3 and 5 month old CKO, heterozygous and wild type eyes revealed that the scotopic a- and b-wave (Fig.1A) and photopic b-wave (Fig.1B) amplitudes were diminished in both the CKO and heterozygous animals, with the CKO most severely affected. CKO eyes had the lowest amplitudes in all ERG tests and were significantly different from wild type (Fig.2A,B and Table 1). When compared to heterozygous eyes, all but two ERG measurements were significantly different (Fig.2A, B and Table 1). As a group the heterozygous eyes were significantly different from WT in all but one measurement (Fig.2A, B and Table 1). Both CKO and heterozygous eyes showed variability in the level of attenuation, consistent with the mosaic expression of the *Chx10Cre* allele (see below). The observed decrease in ERG function in heterozygous mice was unexpected, based on the lack of any detectable immunohistochemical defect in these animals. These data suggest that the proximal cause of such a functional abnormalities may reside in molecular changes affecting phototransduction rather than retinal morphology.

Given the profound abnormality of ERG responses in all the CKO animals tested, and their progressive inability to respond to light, we carried out a morphological analysis of their retinas attempting to establish a correlate between abnormal function and anatomical phenotype.

Chx10Cre expression results in the mosaic inactivation of Dicer in the mouse retina

As previously reported (Rowan and Cepko, 2004), Cre expression from the *Chx10Cre* transgenic allele does not drive cre expression in all retinal cells. As a result, not all cells in CKO retinas would be expected to lack a functional Dicer protein. To determine which retinal cells in CKO animals lacked Dicer, we performed RNA *in situ* hybridizations on retinal sections using a probe that was specific for the floxed exon in the *Dicer* conditional allele (Harris et al., 2006). In wild type retinas, native *Dicer* was expressed in the vast majority of retinal cells (Fig.3 A). Staining in photoreceptors appeared localized in the inner segments. Some cells of the inner nuclear layer and ganglion cell layer were also labeled.

Ganglion cells, possibly because of their abundant cytoplasm, appeared more intensely stained than other cell types.

In the P16 CKO retinas (Figure 3B), *Dicer* expression was found to be patchy, with groups of labeled cells interdigitated with unlabeled cells. For example, cells in the ganglion cell layer were negative in some areas and positive in adjacent regions (Fig.3B). To determine if patchy expression of *Dicer* in CKO retinas was a reflection of the mosaic expression of the *Chx10Cre* driver, we examined Cre expression in CKO animals by means of anti-Cre antibodies. In the retinas of these mice, nuclei of cells in the inner nuclear layer, most likely bipolar cells, were stained as expected (Figure 4). However, the pattern of labeling was not uniform but contained patches of Cre-negative cells contiguous to clusters of Cre-positive cells.

The *cre* gene is fused to GFP, and the fusion is run off the chx10 promoter (Rowan and Cepko, 2004). Therefore, we could also reveal cre-positive cells using anti-GFP antibodies. The pattern of staining obtained with either Cre or GFP antibodies was identical (data not shown). The mosaic expression of *Dicer* in the CKO retinas was also shown by staining for *β-Gal* on retinal sections obtained from mice containing the R26R cre inducible reporter allele (*Chx10Cre*; *R26R; Dicer*^{flox}/*Dicer*^{flox}). The R26R allele allowed for the detection of cells that had undergone a recombination event due to expression of cre recombinase from the *Chx10Cre* transgene (Soriano, 1999) (see supplemental figure S1).

Our data indicate that *Dicer* inactivation using the *Chx10Cre* transgene results in the production of mosaic retinas in which *Dicer* null cells are located adjacent to *Dicer* positive cells.

Mosaic inactivation of Dicer in the retina leads to a decrease in retinal-specific miRNAs

To determine if partial *Dicer* inactivation in CKO retinas resulted in aberrant miRNA processing, we performed a small RNA northern blot for miRNAs known to be expressed specifically in the retina or elsewhere in the CNS (miR-96, miR-124a and miR-204). miR-96 and miR-204 are highly expressed in the developing and adult retina, while miR-124a is expressed throughout the entire CNS (Deo et al., 2006; Karali et al., 2007; Ryan et al., 2006). Northern blots were performed on pooled retinas from control and CKO animals (see Methods).

At 1 month, compared to wild type, the mature form of all three miRNAs examined was not changed (Fig. 5). At three months, mature miR-96 and miR-124 were found to be decreased 70% compared to wild type. At two years, mature miR-96 was decreased 63% and miR-124 was decreased 36%. Interestingly, we observed a decrease in production of mature miR-96 and miR-124 in heterozygous retinas (Fig. 5). The decrease in miRNA levels in heterozygous retinas does not result in a phenotypic defect (see Fig.10B) but may, at least partially, explain why heterozygous animals contained defective ERGs (see Fig. 1 and Fig. 2). A decrease in the number of retina cells, compared to wild type, expressing the retinal-specific microRNA miR-183 was also detected in 7 month-old CKO retinas by means of RNA *in situ* hybridization (see supplemental figure S2).

At all stages examined, miR-204 expression was unchanged (Fig. 5). miR-204 has been reported to be specifically expressed in a subset of cells in the inner nuclear layer of the retina (Deo et al., 2006). The *Chx10cre* allele used in our experiments is expressed in a very mosaic pattern in the inner nuclear layer (see Fig. 4), which may be the cause of our inability to detected alterations in the expression of this particular miRNA in mutant animals. Both miR-124 and miR-96 have been reported to be broadly expressed throughout the retina (Karali et al., 2007;Xu et al., 2007). Upon removal of Dicer from the retina, cells undergo

progressive cell death (see Fig. 9D and Fig. 10A). The increase in mature miRNAs found in Dicer null retinas at the two year time point compared to three months could be due to a decrease in the number of Dicer null cells present in the retina at this late stage.

Retinal phenotype in CKO mice

The most striking abnormal feature present in all CKO retinas aged P16 and older was the presence of photoreceptor rosettes (Figure 6). Rosettes are circular structures, comprising photoreceptors only, that are oriented toward an internal lumen with photoreceptor outer segments protruding inward. Fragments of retinal pigment epithelial cells are also occasionally observed inside rosette lumen (not shown).

In P16 mutants, rosettes were scattered along an otherwise normal retinal outer surface and were primarily composed of photoreceptors and their synaptic terminals (Fig. 6). The number and density of rosettes varied in each retina, however each rosette was separated from the others and clearly identifiable even at low magnification. Interestingly, the presence of rosettes did not appear to alter the typical laminar organization of the retina: inner retinal layers were unperturbed by overlying rosettes and the number of rows of photoreceptor nuclei in areas devoid of rosettes was found to be normal (12–14; data not shown). At this early stage, the presence of rosettes was not accompanied by concomitant overexpression of glial fibrillary acidic protein (GFAP) in Müller cells. GFAP overexpression is a well known indicator of glial activation and is associated with retinal degeneration or perturbation in laminar organization (Marc et al., 2003). In the CKO animals, GFAP overexpression in Müller cells was only detected at later stages during which a clear loss of retinal cells was taking place (Fig 9E).

Rosettes have previously been described in a number of pathological retinal conditions, including retinoblastoma (Yuge et al., 1995); diabetic retinopathy (Lahav et al., 1975) and retinitis pigmentosa (Tulvatana et al., 1999). In these diseases, retinal degeneration and/or abnormal proliferation are present (Lin et al., 2001). To test whether the formation of photoreceptor rosettes in *Dicer* depleted retinas was associated with an increase in cell proliferation in the photoreceptor layer we treated P35 animals with BrdU. In addition, we stained sections from multiple P16 retinal samples with antibodies against phosphohistone H3, a specific marker of cell proliferation (Dhomen et al., 2006; Fig. 7). Using either method, we failed to detect dividing cells in CKO retinas, although we observed, as expected, mitotic cells in other ocular tissues such as the cornea (Fig. 7). Thus rosette formation did not appear to be caused by an upregulation in retinal cell proliferation.

To determine if areas of rosette formation were those that had experienced Cre expression, tissue samples were labeled with anti-Cre antibodies. Rosettes were found in areas where bipolar cells expressed cre suggesting that these structured formed as a result of a decrease in miRNA levels (Fig.7).

Developmental observations in Dicer CKO retinas

Appropriate formation of retinal layers depends critically upon the maintenance of apico-basal polarity in the neuroepithelial cells during early development. Retinal neuroblasts are joined by junctional complexes precisely positioned at the apico-basolateral domain of the cell membrane. Alterations of the molecular components controlling these complexes lead to abnormal retinal layering and subsequent rosette formation (Erdmann et al., 2003; Malicki et al., 2003; Masai et al., 2003; reviewed in Malicki, 2004; Galli-Resta et al., 2008). To test the hypothesis that the rosettes observed in Dicer CKO mature retinas could be caused by major defects in the apico-basal polarity of neuroepithelial cells, we examined by ICCH and electron microscopy (EM) CKO and wt retinas at 2 days of age (n=8 animals for each

genotype). We assessed a) early retinal layering; b) laminar position of dividing and differentiating cells and; c) position of junctional complexes among differentiating photoreceptors and neuroblasts. Results are illustrated in supplemental figure S3 and supplemental figure S4.

This analysis demonstrated that immature Dicer CKO retinas did not contain major defects in neuroepithelial cell polarity or in the structure of adherens junctions, therefore indicating that rosettes, which are found in older mutant retinas, were not the result of improper patterning of these cell types.

Characterization of cell types in CKO retinas

The normal complement of retinal cell types, comprising neurons and glia, (i.e. Jeon et al., 1998; Haverkamp and Wassle, 2000, etc.), were represented in the CKO retinas from P16 onwards. Cells were observed to occupy the expected laminar positions and the overall retinal architecture appeared normal. One exception, as discussed above, was the presence of rosettes at all stages examined. Using cell-type specific antibodies all major cell types including rods and cones (Fig.8A), horizontal cells (Fig.8B), rod and cone bipolar cells (Fig. 8C, D), various types of amacrine cells (Fig.8E) and ganglion cells (Fig.8F) were present in CKO retinas. All cells displayed normal morphology, pattern of stratification and appropriate lamination in the plexiform layers. Retinal glial cells, in particular astrocytes and Müller cells (Fig.7A and B), were also appropriately represented and positioned correctly in the CKO retinas.

The majority of rod bipolar cells were Cre-positive, as demonstrated by anti-Cre (Fig.8C) and anti-GFP antibodies (not shown). As expected, Cre staining was nuclear and showed a similar pattern in the CKO and wt retinas (Fig.4A and B). Cre-positive nuclei occupied the presumptive bipolar layer, and thus both rod and cone bipolar cells were Cre-positive and presumably Dicer null. A few nuclei from Cre-positive, PKCα-negative cells were larger in size and were presumably derived from Müller cells.

Using cell type specific antibodies, the data suggested that removal of Dicer in retinal progenitors and differentiated bipolar cells did not affect retinal cell fate or migration of cells to their wild type locations during retinal development.

From rosette formation to retinal degeneration in Dicer depleted retinas

The time period from P16 to P45 was characterized by progressive alteration and remodeling of the laminar retinal structure in CKO mice (Fig. 9). The number of rosettes increased (Fig.9A) while their structure became more complex: bipolar and horizontal cells penetrated the rosettes while photoreceptor clusters were displaced toward the outer retina (Fig. 9). The normal synaptic structures of the OPL also became displaced toward the outer retina (Fig.9A, B); concomitantly, the dendrites of both rod bipolar and horizontal cells sprouted profusely in the direction of the photoreceptors (Fig.9C–E). Entire retinal domains appeared to be displaced outward, resulting in a progressive destruction of the external lamination of the P45 CKO retina. Most dramatically, PSD95, a marker of photoreceptor synaptic terminals, was expressed ectopically in the outer retina and reached the outer limiting membrane (Fig.9A).

As CKO animals reached 3 months of age, the rosettes were observed to decrease in size and eventually disappear from the retina. Photoreceptors composing these rosettes degenerated and the outer nuclear layer became progressively thinner. This was confirmed by detection of pycnotic nuclei in the outer and inner retina by using DNA-binding dyes (Fig.10A). At 3 months, most rosettes had been lost and replaced by areas of extensive degeneration. Generally, the outer nuclear layer appeared to be more reproducibly thinner in the peripheral

as compared to the central retina, suggesting that the degenerative processes had a periphery-to-central gradient. At 3 months of age, in the extreme periphery, the outer nuclear layer was reduced at 2–3 rows (Fig.9F).

Concomitant with outer retinal degeneration, the inner retina also deteriorated and exhibited cellular loss. Simultaneously, Müller cells became hypertrophic with their radial processes increasing in size and GFAP reactivity raising visibly, indicating a generalized glial activation (Fig.9F). At the same time, Cre positive cells became scarce, most likely because a large fraction of these Dicer null cells degenerated, as demonstrated by the progressive thinning of the inner nuclear layer. Surviving rod bipolars often occurred in clusters and had altered morphologies with axonal arborizations that were hypertrophic with enlarged, bulbous like endings and dendrites that were scant and thicker than normal. PKCα staining was abnormally bright and had an unusually punctate appearance. Most of the residual rod bipolar cells were Cre-negative (Fig.9D) and therefore most likely originated from precursors in which Dicer was not inactivated due to the mosaic activity of the *Chx10Cre* transgenic allele (Rowan and Cepko 2004).

Heterozygous animals—Retinas of animals in which a single copy of Dicer was inactivated in the retina (heterozygous animals) were examined by *in situ* hybridization, immunocytochemistry and detailed confocal microscopy. Using these assays, no major defects were detected (Figure 10). However, ERG recordings and Northern blot analysis (see above) did reveal functional abnormalities and a decrease in retinal miRNAs.

Discussion

The role miRNAs play in the development and maintenance of the nervous system is unknown. *Dicer*-deficient zebrafish exhibit abnormal morphogenesis and widespread abnormalities in neural development (Giraldez et al. 2005). However, many aspects of early embryonic development, including patterning and cell fate specification are largely unaffected by *Dicer* deletion in zebrafish, in part due to the inheritance of maternal Dicer. *Dicer*-deficient mice die during early development, around embryonic day 7.5, and were found to be depleted of pluripotent embryonic stem cells (Bernstein et al. 2003). In the mouse nervous system, depletion of *Dicer* in Purkinje cells has been reported to result in neuronal degeneration (Schaefer et al., 2007).

The results reported here highlight the crucial role *Dicer* and miRNAs play in the long-term regulation of retinal cell lamination, survival and function. We have shown that removal of *Dicer* in the mouse retina had no visible impact on early postnatal retinal structure and function since retinal lamination appeared normal and all expected retinal cell types were represented. In addition, the relative widths of the various retinal layers appeared to be very similar between CKO and wild type retinas, although the perturbation to outer retinal surface in the vicinity of photoreceptor rosettes and the mosaic expression of the *Dicer* allele with alternation of normal and abnormal retinal patches, made it virtually impossible to perform histograms of cell distributions. However, by 1 month of age the response to light was significantly diminished and an abnormal retinal lamination clearly detectable.

It is important to note that the *Cre* allele used in these experiments, *Chx10Cre*, drives Cre expression in the retina during embryogenesis. In both lung (Harris et al., 2006) and limb (Harfe et al., 2005) loss of *Dicer* resulted in a substantial decrease of all miRNAs examined ~2 days after Cre expression. In our experiments in the retina, *Dicer* was removed more than 20 days prior to ERG analysis and morphological detection of rosettes at P16.The presence of mature miRNAs at wild type levels 1 month after birth indicates that either miRNAs in the retina are extremely stable or that an additional protein can compensate for

DICER function in this tissue during early postnatal life. This is in stark contrast to what was observed in the mouse limb where *Dicer* removal almost immediately resulted in massive cell death (Harfe et al., 2005). The persistence of mature miRNAs in the Dicer CKO retina might explain the late degeneration of retina cells observed in our experiments.

As CKO animals aged, we observed numerous defects in retinal structure including cell death. These observations suggest that miRNAs are initially required for the retina's ability to respond to light, but not for cell survival. However, miRNAs play an essential role in maintaining the majority of cell types found in the adult retina.

Surprisingly, the light response deficit was observed in heterozygous in addition to homozygous animals suggesting that the level of Dicer protein was essential for proper function of the mouse retina. The light response defect was observed in all ages of retinas lacking a single *Dicer* allele although we could detect no morphological defects in the retina of these heterozygous animals at any stage of life. These data suggest that either the mouse retina is extremely sensitive to the amount of mature miRNAs present or that *Dicer* has additional, non-miRNA functions in the mouse retina (see below). To our knowledge, this is the first demonstration in which the dosage of Dicer protein within a cell influences function. This light response deficit seen in heterozygote animals suggests one or more elements of the phototransduction cascade itself may be affected, since alteration here would likely quickly affect the ERG response but not retinal structure in the short term.

It is possible that not all the phenotypes we observed upon removal of *Dicer* in the retina were due to the loss of mature miRNAs. *Dicer* could be processing other double-stranded RNAs besides miRNAs within the targeted retinal cells. In addition, this enzyme could play a role in the nucleus as suggested by loss of centromeric and pericentromeric silencing in *Dicer* null ES cells (Murchison et al., 2005; Kanellopoulou et al., 2005).

Given the fact that the first sign of morphological abnormality in CKO retinas was the formation of photoreceptor rosettes and that photoreceptor function was affected early, our data suggest that photoreceptors are the retinal cell type most sensitive to an imbalance in the production and maturation of miRNAs.

Photoreceptor rosettes are a common finding in a variety of retinal diseases. In particular, they are found in diabetic retinopathy, retinitis pigmentosa and ischemia (Lahav et al., 1975; Yuge et al., 1995; Tulvatana et al., 1999). Rosettes have also been reported to result from decreased levels of secreted proteins of the Wnt family, shown to function as organizers of retinal lamination. Rosette formation is usually associated with alteration of cytoskeleton, abnormal production of extracellular matrix and adhesion molecules (Li and Sakaguchi, 2004; Lunardi et al., 2006) in a variety of vertebrates, including Xenopus, zebrafish, chicken, mice and humans.

Despite the fact that the exact trigger of rosette formation is not known, this common abnormality in retinal lamination might be caused early in development through alterations in polarity of neuroblasts (reviewed in Malicki, 2004). To test this hypothesis, we compared wt and Dicer CKO retinas at two days of age, a time at which inner retinal layers are partially formed and the outer retina is still largely composed of neuroblasts and differentiating photoreceptors (Sharma et al., 2003). Morphological examinations of retinal sections by ICCH and EM, aimed at assessing the proper orientation and polarity of neuroblasts, mitotic cells, developing photoreceptors and laminar position of differentiated cells, did not reveal major abnormalities. Adherens junctions in particular were found at their appropriate location at the outer retinal margin between differentiating photoreceptors and neuroblasts. These data were consistent with our observation that wild type amounts of miRNAs were found during early postnatal development. Hence, it appears that rosette

formation in the Dicer KO retina is not linked to major changes in neuroblast polarity or cell orientations and instead occurs upon completion of retinal development.

Rosette formation may be followed by progressive photoreceptor death (Lin et al., 2001). This is similar to what we observed upon removal of *Dicer* in the retina. While the pattern of cell degeneration observed in mouse Purkinje cells upon *Dicer* inactivation (Schaefer et al., 2007) bears similarity to neurodegenerative disorders such as Alzheimer's and Parkinson's disease, the pattern of retinal degeneration reported here does not precisely parallel genetically well understood forms of inherited retinal disease, such as Retinitis Pigmentosa. In both the human disease and in mouse models of this disorder, a clear rod-cone degeneration is observed first, while the degeneration of inner neurons, including horizontal and bipolar cells, is usually secondary (Gargini et al., 2007). This partially reflects the fact that the primary genetic defects typically occurs in a photoreceptor-specific gene. In the Dicer CKO retina examined here, cellular death after P30 affected both rod and cone cell function simultaneously and was accompanied by a concomitant decrease in the number of second order neurons. Interestingly, rod bipolar cells that persisted in retinas aged 3 months and older were also Cre-negative. Albeit their morphology was abnormal, the fact that these cells survived longer than Dicer null rod bipolars suggests the occurrence of cell autonomous events in the genesis of the complex CKO phenotype.

At least 78 of the >400 miRNAs reported in mice are expressed in the retina (Xu et al., 2007). Since each miRNA could potentially regulate hundreds of genes, it is unclear what the role individual miRNAs may play in retinal development during embryonic and postnatal life. To unravel the exact role miRNAs play in rosette formation and/or ERG loss, the conditional removal of miRNAs specifically expressed in the retina, such as miR-183 (Karali et al., 2007), could be attempted.

Inactivation of *Dicer* in the mouse model used here likely resulted in a decrease in global levels of most retinal-expressed miRNAs. The unique pattern of retinal degeneration uncovered in this report is the first step towards identifying the overall role miRNAs contribute to retinal cell function and survival. Our results provide insight into the molecular mechanisms of retinal degeneration and the maintenance of normal retinal function and architecture.

Supplementary Material

Refer to Web version on PubMed Central for supplementary material.

Acknowledgments

Funded by grant NIH R01 EY12654 (ES); EY011123, EY008571, EY13729, EY007132 and NS36302 and grants from the MVRF, FFB and JDRF, and from RPB (WH & JA); Howard Hughes Medical Institute and NIH EY0 9676 (CC); NIH Grant R03-DA22201(MTM); UF start-up funds (BDH).

References

Ambros V. MicroRNA pathways in flies and worms: growth, death, fat, stress, and timing. Cell. 2003; 113:673–676. [PubMed: 12809598]

Ambros V, Chen X. The regulation of genes and genomes by small RNAs. Development. 2007; 134:1635–1641. [PubMed: 17409118]

Babak T, Zhang W, Morris Q, Blencowe BJ, Hughes TR. Probing microRNAs with microarrays: tissue specificity and functional inference. RNA. 2004; 10:1813–1819. [PubMed: 15496526]

Barad O, Meiri E, Avniel A, Aharonov R, Barzilai A, Bentwich I, Einav U, Gilad S, Hurban P, Karov Y, Lobenhofer EK, Sharon E, Shiboleth YM, Shtutman M, Bentwich Z, Einat P. MicroRNA

expression detected by oligonucleotide microarrays: system establishment and expression profiling in human tissues. Genome Res. 2004; 14:2486–2494. [PubMed: 15574827]

Bernstein E, Kim SY, Carmell MA, Murchison EP, Alcorn H, Li MZ, Mills AA, Elledge SJ, Anderson KV, Hannon GJ. Dicer is essential for mouse development. Nat Genet. 2003; 35:215–217. [PubMed: 14528307]

Cao X, Yeo G, Muotri AR, Kuwabara T, Gage FH. Noncoding RNAs in the mammalian central nervous system. Annu Rev Neurosci. 2006; 29:77–103. [PubMed: 16776580]

Close JL, Gumuscu B, Reh TA. Retinal neurons regulate proliferation of postnatal progenitors and Müller glia in the rat retina via TGF beta signaling. Development. 2005; 132:3015–3026. [PubMed: 15944186]

Cuellar T, Davis T, Loeb G, Nelson PT, Harfe BD, Ullian E, McManus MT. Dicer loss in striatal neurons produces behavioral and neuroanatomical phenotypes in absence of neurodegeneration. PNAS. 2008 in press.

Davis TH, Cuellar TL, Koch S, Barker A, Harfe B, McManus MT, Ullian E. Conditional loss of Dicer disrupts cellular and tissue morphogenesis in the cortex and hippocampus. J Neurosci. 2008 in press.

Dhomen NS, Balaggan KS, Pearson RA, Bainbridge JW, Levine EM, Ali RR, Sowden JC. Absence of chx10 causes neural progenitors to persist in the adult retina. Invest Ophthalmol Vis Sci. 2006; 47:386–396. [PubMed: 16384989]

Erdmann B, Kirsch FP, Rathjen FG, More MI. Ncadherin is essential for retinal lamination in the zebrafish. Dev Dyn. 2003; 226:570–577. [PubMed: 12619142]

Galli-Resta L, Leone P, Bottari D, Ensini M, Rigosi E, Novelli E. The genesis of retinal architecture: an emerging role for mechanical interactions? Progr Ret Eye Res. 2008 (in the press).

Gargini C, Terzibasi E, Mazzoni F, Strettoi E. Retinal organization in the retinal degeneration 10 (rd10) mutant mouse: a morphological and ERG study. J Comp Neurol. 2007; 500:222–238. [PubMed: 17111372]

Giraldez AJ, Cinalli RM, Glasner ME, Enright AJ, Thomson JM, Baskerville S, Hammond SM, Bartel DP, Schier AF. MicroRNAs regulate brain morphogenesis in zebrafish. Science. 2005; 308:833–838. [PubMed: 15774722]

Harfe BD, McManus MT, Mansfield JH, Hornstein E, Tabin CJ. The RNaseIII enzyme Dicer is required for morphogenesis but not patterning of the vertebrate limb. Proc Natl Acad Sci U S A. 2005; 102:10898–10903. [PubMed: 16040801]

Harris KS, Zhang Z, McManus MT, Harfe BD, Sun X. Dicer function is essential for lung epithelium morphogenesis. Proc Natl Acad Sci U S A. 2006; 103:2208–2213. [PubMed: 16452165]

Haverkamp S, Wassle H. Immunocytochemical analysis of the mouse retina. J Comp Neurol. 2000; 424:1–23. [PubMed: 10888735]

Kanellopoulou C, Muljo SA, Kung AL, Ganesan S, Drapkin R, Jenuwein T, Livingston DM, Rajewsky K. Dicer-deficient mouse embryonic stem cells are defective in differentiation and centromeric silencing. Genes & Devel. 2005; 19:489–501. [PubMed: 15713842]

Karali M, Peluso I, Marigo V, Banfi S. Identification and characterization of microRNAs expressed in the mouse eye. Invest Ophthalmol Vis Sci. 2007; 48:509–515. [PubMed: 17251443]

Jadhav AP, Cho SH, Cepko CL. Notch activity permits retinal cells to progress through multiple progenitor states and acquire a stem cell property. Proc Natl Acad Sci U S A. 2006; 103:18998–19003. [PubMed: 17148603]

Jeon CJ, Strettoi E, Masland RH. The major cell populations of the mouse retina. J Neurosci. 1998; 18:8936–8946. [PubMed: 9786999]

Lagos-Quintana M, Rauhut R, Yalcin A, Meyer J, Lendeckel W, Tuschl T. Identification of tissue-specific microRNAs from mouse. Curr Biol. 2002; 12:735–739. [PubMed: 12007417]

Lahav M, Albert DM, Craft JL. Light and electron microscopic study of dysplastic rosette-like structures occurring in the disorganized mature retina. Albrecht Von Graefes Arch Klin Exp Ophthalmol. 1975; 195:57–68. [PubMed: 167600]

Lewis BP, Burge CB, Bartel DP. Conserved seed pairing, often flanked by adenosines, indicates that thousands of human genes are microRNA targets. Cell. 2005; 120(1):15–20. Jan 14. [PubMed: 15652477]

Li M, Sakaguchi DS. Inhibition of integrin-mediated adhesion and signaling disrupts retinal development. Dev Biol. 2004; 275:202–214. [PubMed: 15464583]

Lin SC, Skapek SX, Papermaster DS, Hankin M, Lee EY. The proliferative and apoptotic activities of E2F1 in the mouse retina. Oncogene. 2001; 20:7073–7084. [PubMed: 11704831]

Lunardi A, Cremisi F, Dente L. Dystroglycan is required for proper retinal layering. Dev Biol. 2006; 290:411–420. [PubMed: 16406325]

Malicki J. Cell fate decisions and patterning in the vertebrate retina: the importance of timing, asymmetry, polarity and waves. Curr Opin Neurobiol. 2004; 14:15–21. [PubMed: 15018933]

Malicki J, Jo H, Pujic Z. Zebrafish N-cadherin, encoded by the glass onion locus, plays an essential role in retinal patterning. Dev Biol. 2003; 259:95–108. [PubMed: 12812791]

Marc RE, Jones BW, Watt CB, Strettoi E. Neural remodeling in retinal degeneration. Prog Retin Eye Res. 2003; 22:607–655. [PubMed: 12892644]

Masai I, Lele Z, Yamaguchi M, Komori A, Nakata A, Nishiwaki Y, Wada H, Tanaka H, Nojima Y, Hammerschmidt M, Wilson SW, Okamoto H. N-cadherin mediates retinal lamination, maintenance of forebrain compartments and patterning of retinal neurites. Development. 2003; 130:2479–2494. [PubMed: 12702661]

Miska EA, Alvarez-Saavedra E, Townsend M, Yoshii A, Sestan N, Rakic P, Constantine-Paton M, Horvitz HR. Microarray analysis of microRNA expression in the developing mammalian brain. Genome Biol. 2004; 5:R68. [PubMed: 15345052]

Murchison EP, Partridge JF, Tam OH, Cheloufi S, Hannon GJ. Characterization of Dicer-deficient murine embryonic stem cells. PNAS. 2005; 102:12135–12140. [PubMed: 16099834]

Nakagawa S, Takada S, Takada R, Takeichi M. Identification of the laminar-inducing factor: Wnt-signal from the anterior rim induces correct laminar formation of the neural retina in vitro. Dev Biol. 2003; 260:414–425. [PubMed: 12921742]

O'Rourke JR, Georges SA, Seay HR, Tapscott SJ, McManus MT, Goldhamer DJ, Swanson MS, Harfe BD. Essential role for Dicer during skeletal muscle development. Dev Biol. 2007; 311:359–368. [PubMed: 17936265]

Rowan S, Cepko CL. Genetic analysis of the homeodomain transcription factor Chx10 in the retina using a novel multifunctional BAC transgenic mouse reporter. Dev Biol. 2004; 271:388–402. [PubMed: 15223342]

Ryan DG, Oliveira-Fernandes M, Lavker RM. MicroRNAs of the mammalian eye display distinct and overlapping tissue specificity. Mol Vis. 2006; 12:1175–1184. [PubMed: 17102797]

Sempere LF, Freemantle S, Pitha-Rowe I, Moss E, Dmitrovsky E, Ambros V. Expression profiling of mammalian microRNAs uncovers a subset of brain-expressed microRNAs with possible roles in murine and human neuronal differentiation. Genome Biol. 2004; 5:R13. [PubMed: 15003116]

Sharma RK, O'Leary TE, Fields CM, Johnson DA. Development of the outer retina in the mouse. Brain Res Dev Brain Res. 2003; 145:93–105.

Schaefer A, O'Carroll D, Tan CL, Hillman D, Sugimori M, Llinas R, Greengard P. Cerebellar neurodegeneration in the absence of microRNAs. Exp Med. 2007; 204:1553–1558.

Soriano P. Generalized lacZ expression with the ROSA26 Cre reporter strain. Nat Genet. 1999; 21(1): 70–71. [PubMed: 9916792]

Thomson JM, Parker J, Perou CM, Hammond SM. A custom microarray platform for analysis of microRNA gene expression. Nat Methods. 2004; 1:47–53. [PubMed: 15782152]

Tulvatana W, Adamian M, Berson EL, Dryja TP. Photoreceptor rosettes in autosomal dominant retinitis pigmentosa with reduced penetrance. Arch Ophthalmol. 1999; 117:399–402. [PubMed: 10088824]

Xu S, Witmer PD, Lumayag S, Kovacs B, Valle D. MicroRNA (miRNA) transcriptome of mouse retina and identification of a sensory organ-specific miRNA cluster. J Biol Chem. 2007; 282:25053–25066. [PubMed: 17597072]

Yuge K, Nakajima M, Uemura Y, Miki H, Uyama M, Tsubura A. Immunohistochemical features of the human retina and retinoblastoma. Virchows Arch. 1995; 426:571–575. [PubMed: 7655737]

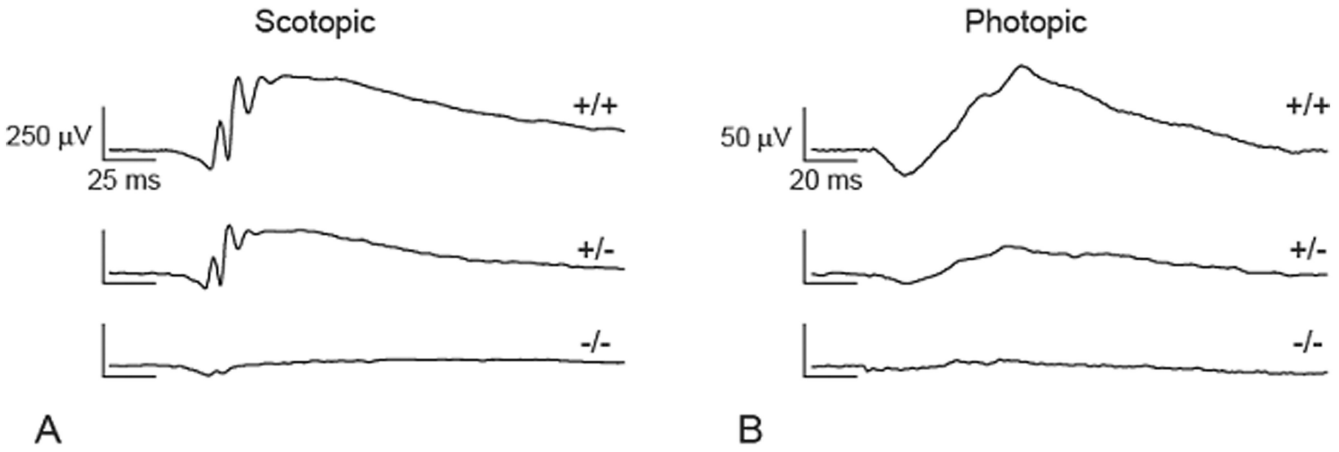

Figure 1.

Representative scotopic (A) and corresponding photopic (B) ERG traces recorded at 5 months of age from wild type (WT), Dicer CKO heterozygous (here indicated as +/−), and Dicer CKO homozygous (here indicated as −/−). Traces from each strain were similar at all time points analyzed.

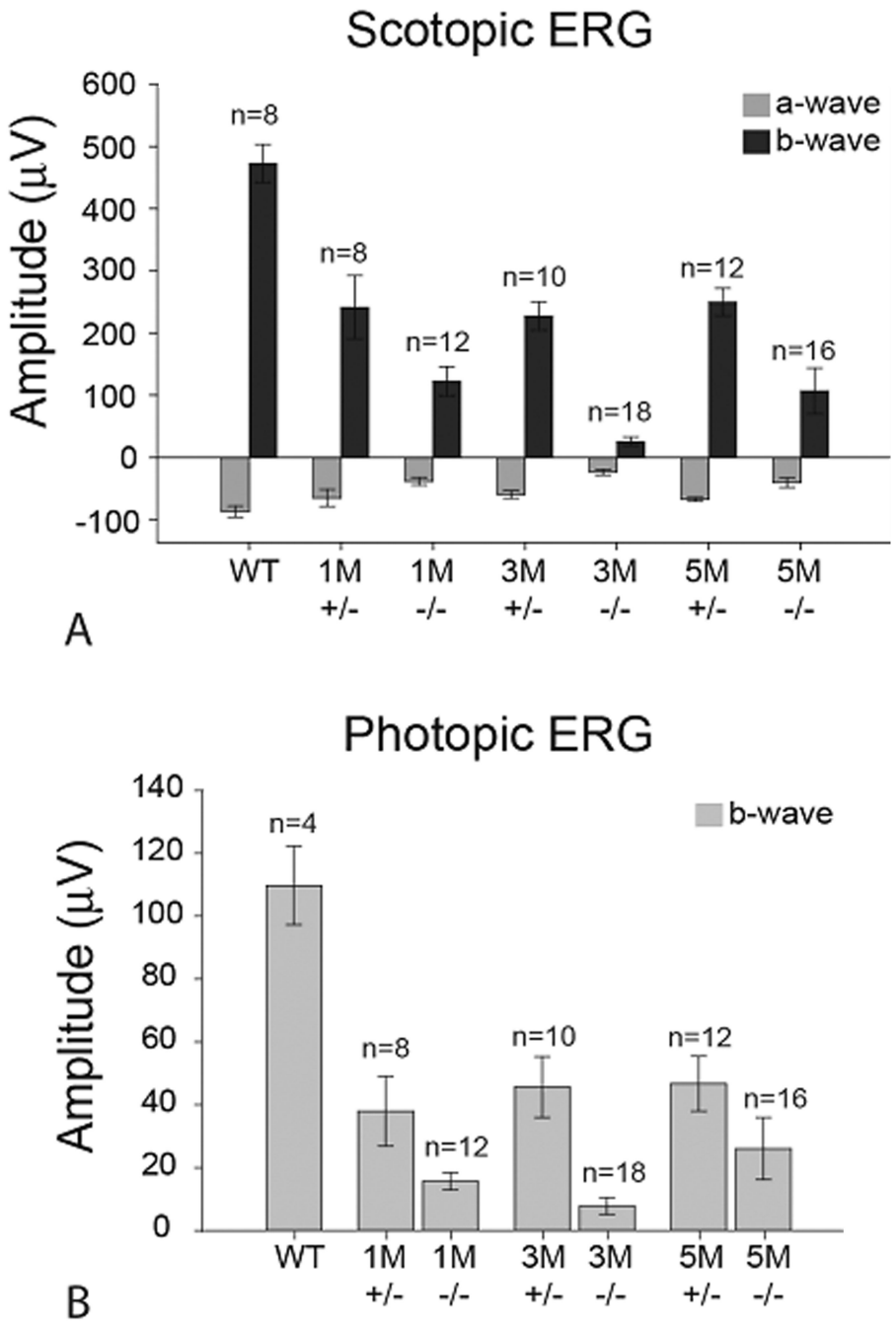

Figure 2.

Average maximum scotopic a- and b-wave (A) and photopic b-wave (B) amplitudes for wild-type (WT), Dicer +/−, and Dicer −/− eyes. (A) Scotopic values for Dicer +/− and Dicer −/− at 1, 3, and 5 months differed from wild-type and each other, with the exception of the 1 month a-wave value for the Dicer +/−. (B) Photopic values for Dicer +/− and Dicer −/− eyes at 1, 3, and 5 months differed from wilt-type and each other, with the exception of the 5 month b-wave value between the Dicer +/− and Dicer −/−. Different sets of mice were recorded at 1, 3, and 5 months, as the mice were sacrificed the day after ERG for morphological studies.

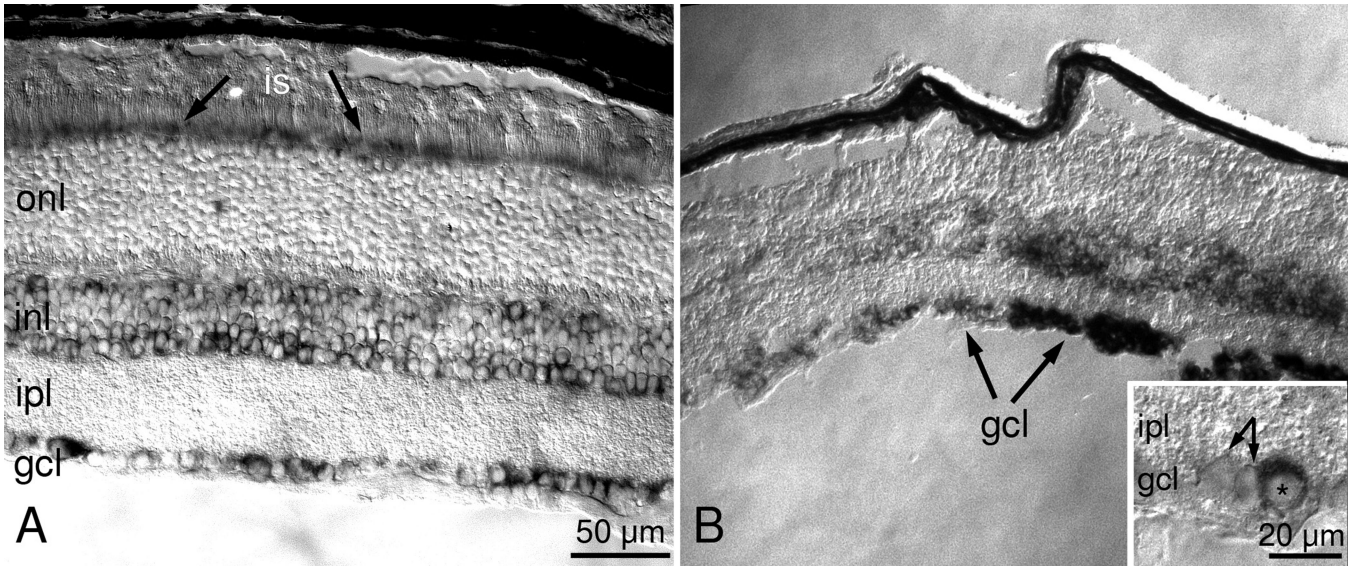

Figure 3.

In situ hybridization for Dicer in wt (A) and CKO (B) retinas at P16. In the wt animal, virtually all retinal cell types were labeled. Photoreceptor staining was concentrated within the inner segments (is, arrows) that contains the protein synthetic machinery, while the outer nuclear layer (onl), mostly containing their nuclei, was devoid of staining. The cytoplasm of cells of the inner nuclear layer (inl) and ganglion cell layer (gcl) also showed intense Dicer expression. In the CKO (B), expression was more patchy than in the wild type. Most photoreceptors were negative, while cells in the ganglion cell layer (gcl) were either very intensely or relatively weakly stained (arrows). The inset shows a high magnification of the stained cells in the gcl. Arrows point to the somas of two negative cells adjacent to a larger cell, darkly stained (asterisk), all presumably ganglion cells. ipl: inner plexiform layers.

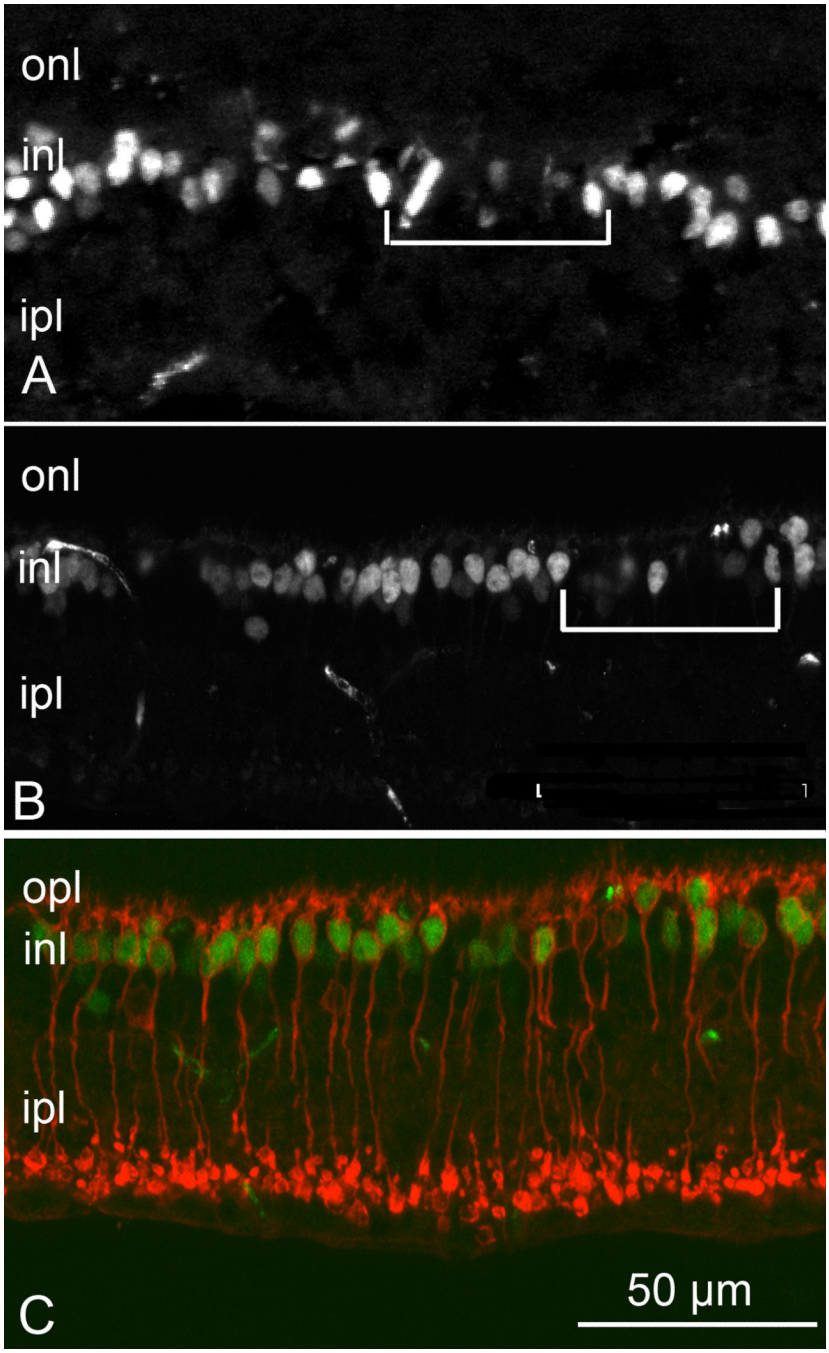

Figure 4.

Immunofluorescence staining with Cre antibodies in the CKO retina (A) showing patchy expression of the transgene. Patchy expression was also observed in the wt retina (B). Cre-negative cells (within the brackets) alternated with Cre-positive, fluorescent nuclei in the inner nuclear layer at the presumptive location of bipolar cells. (C) Immunostaining for Cre (green) and PKCalpha (red) for rod bipolar cells. With few exceptions, rod bipolar cells were Cre-positive. onl: outer nuclear layer; opl: outer plexiform layer; inl: inner nuclear layer; ipl: inner plexiform layer.

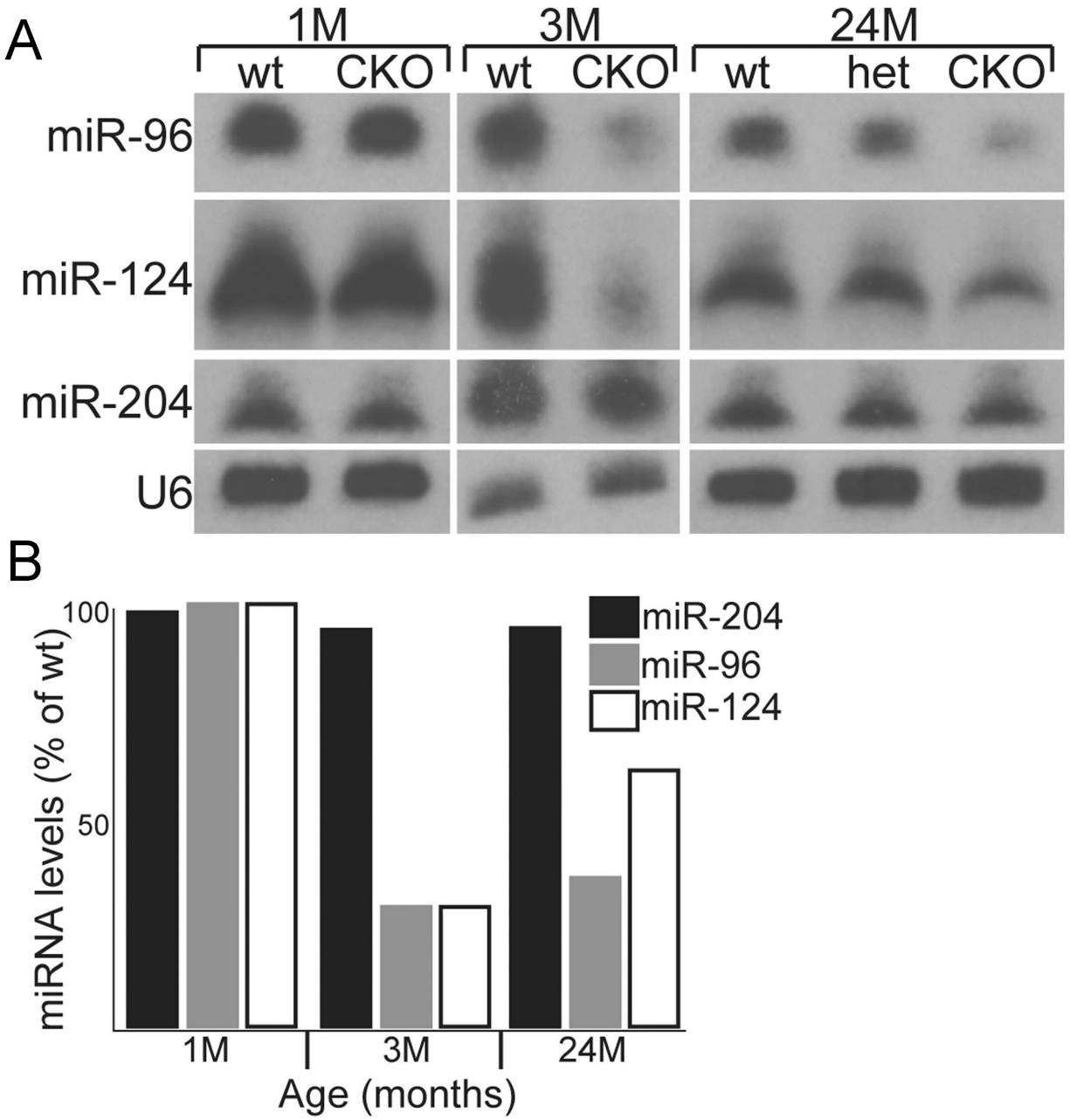

Figure 5.

Northern blot analysis of mature miRNA levels from retinal homogenates of wt, heterozygous and mutant animals. A: Northern Blot analysis of equal amounts of RNA obtained from pooled samples of wild type, mutant and, at the 24-month time point, heterozygous retinas (see Methods). The small RNA U6 was used as a loading control. B: Histogram of the relative expression levels for each miRNA examined on the Northern Blot show in “A”. At the 24-month time point, miR-96 and miR-124a were decreased 18% and 10%, respectively in heterozygous retinas. No decrease in miR-204 expression was observed at any time point examined (see text). Expression levels were normalized to wild type as described in the Methods.

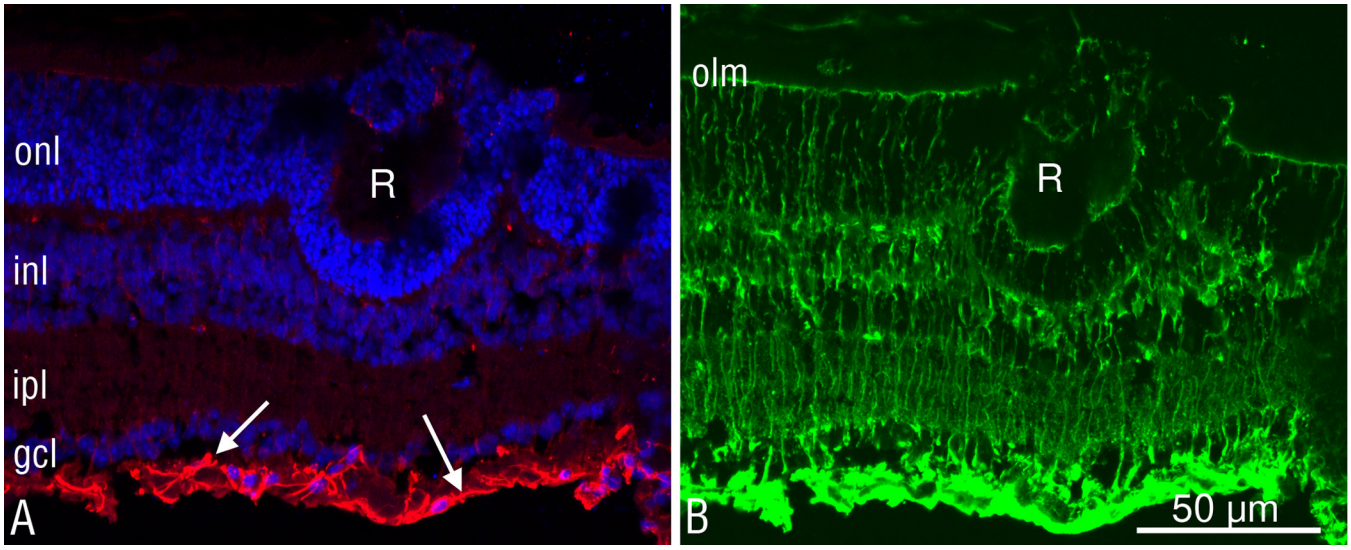

Figure 6.

Representative rosette in a P16 Dicer CKO retinal section. A: Nuclear staining (blue) demonstrated that the rosette (R) at this stage of development was composed exclusively of photoreceptors (identified by their distinctive nuclear morphology). GFAP staining (red) was limited to astrocytic processes in the ganglion cell layer (arrows) indicating that macroglial reactivity was virtually absent upon removal of *Dicer*. Rosettes did not appear to contain Müller cells since the Müller cell specific enzyme glutamine synthase (green signal in B) did not co-localize with cells in the rosette. olm: outer limiting membrane; onl: outer nuclear layer; inl: inner nuclear layer; ipl: inner plexiform layer; gcl: ganglion cell layer.

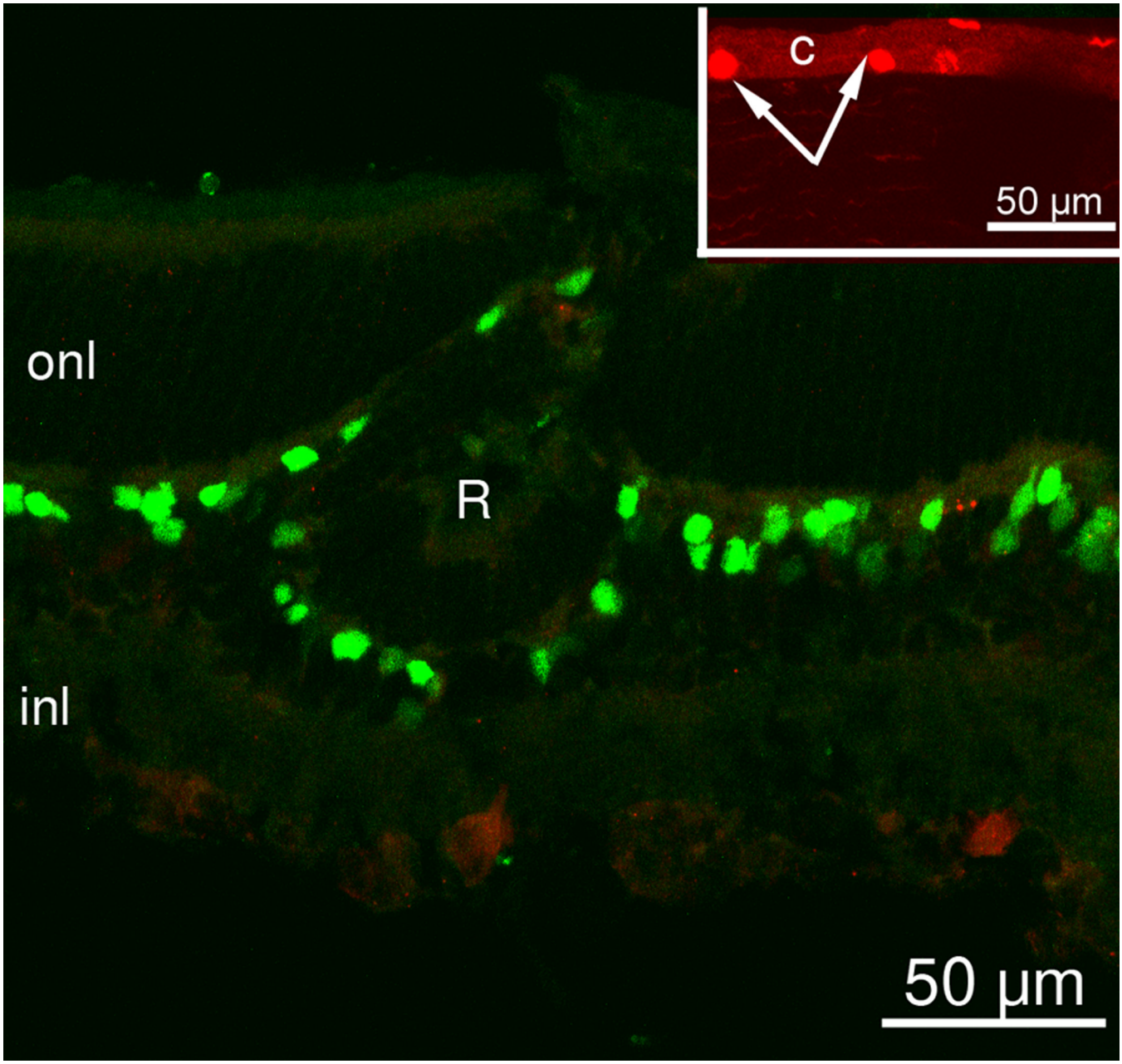

Figure 7.
Vertical section of a P16 CKO retina, exhibiting a typical rosette (R), stained with antibodies against Cre (green) and phosphohistone H3 (red) to locate mitotic cells. No dividing (red) cells were visible. As positive control, the inset shows mitotic cells of the corneal surface (C) from the same ocular section from which the retinal slide was obtained. onl: outer nuclear layer; inl: inner nuclear layer.

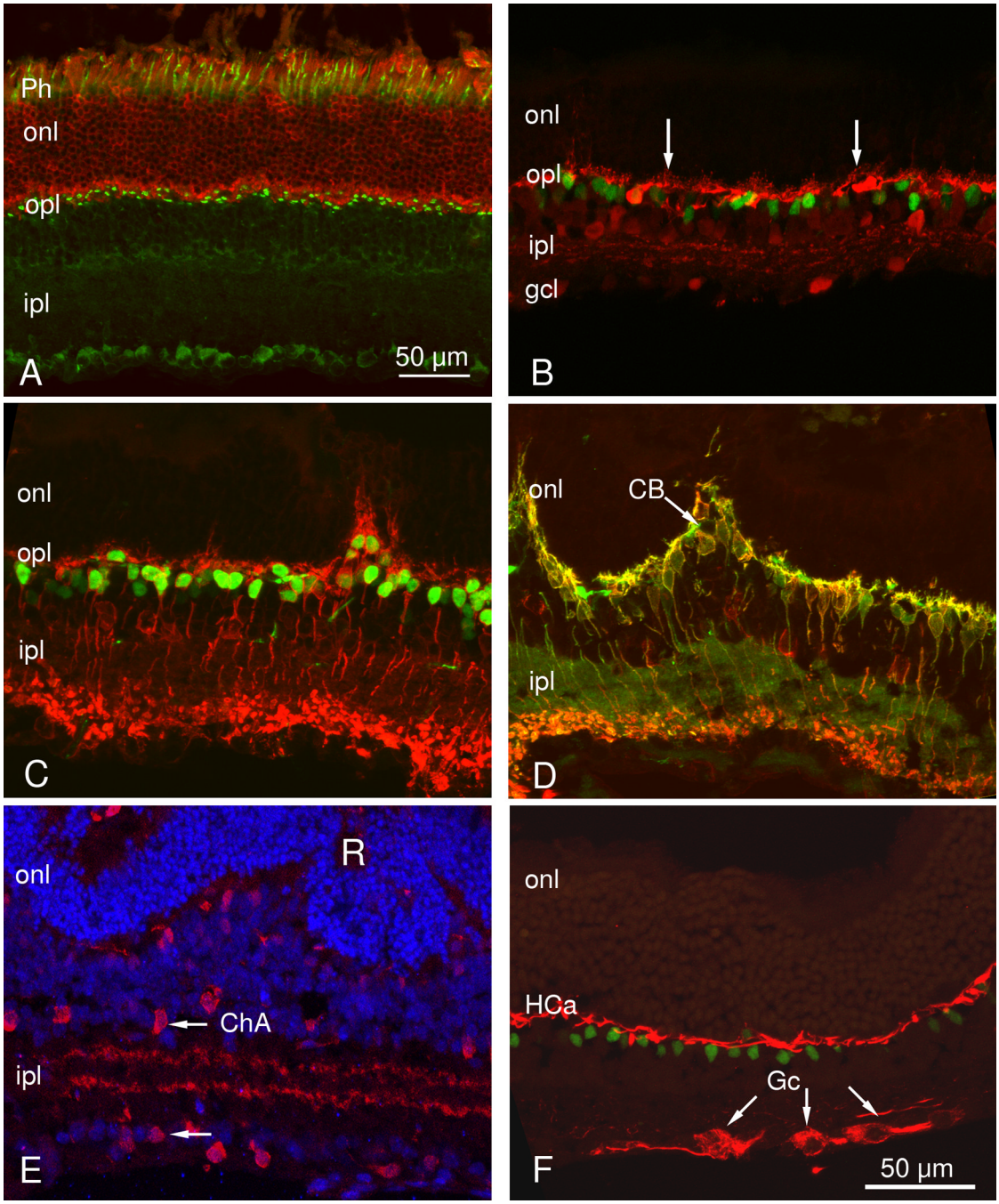

Figure 8.

Characterization of cell types in the CKO retina.

A: Rods and cones, labeled red by recoverin antibody, in a three month-old CKO retina; cones are counterstained green with peanut lectin. Their synaptic terminals formed a regular row in the outer plexiform layer, similar to what is observed in a normal retina.

B: Horizontal cells, labeled red by calbindin D antibody, formed a tier in the outer part of the inner nuclear layer. Some of these sprouted ectopic neuritis toward the outer retina. Green signal denotes Cre staining. Section is from a P35 retina. C: Cre-positive nuclei (green) belong mostly to rod bipolar cells, whose membrane is appropriately labeled red by antibody against PKCα. Section is from a P45 retina.

D: anti-G0α antibodies (green) label ON-centre cone and rod bipolar cells. PKCα antibody labels only rod bipolar cells (red). In this section, orange-yellow cells have been labeled by both antibodies and are therefore rod bipolar cells. Green cells are ON-centre cone bipolar cells (CB). Some of these cells (arrow) appeared displaced toward the outer retina at a location adjacent to a photoreceptor rosette. Section is from a P45 retina.
E: Cholinergic amacrine cells (ChA, red) are seen in the CKO retina at the expected location. Their cell bodies formed two, mirror symmetric populations (arrows) in the inner nuclear and ganglion cell layers, respectively, while their processes formed two bands in the ipl, characteristic to what is observed in the normal retina. Blue staining is a nuclear dye. Section is from a P30 retina.
F: Antibodies against the 200 kDa subunit of neurofilaments (red) revealed the axonal arborizations of horizontal cells (HCa) and the somata of large ganglion cells (Gc) in the appropriate retinal layers. Green cells are stained with Cre-antibodies. Section is from a P35 retina.
Ph: photoreceptors; onl: outer nuclear layer; opl: outer plexiform layer; layer; ipl: inner plexiform layer; gcl: ganglion cell layer.

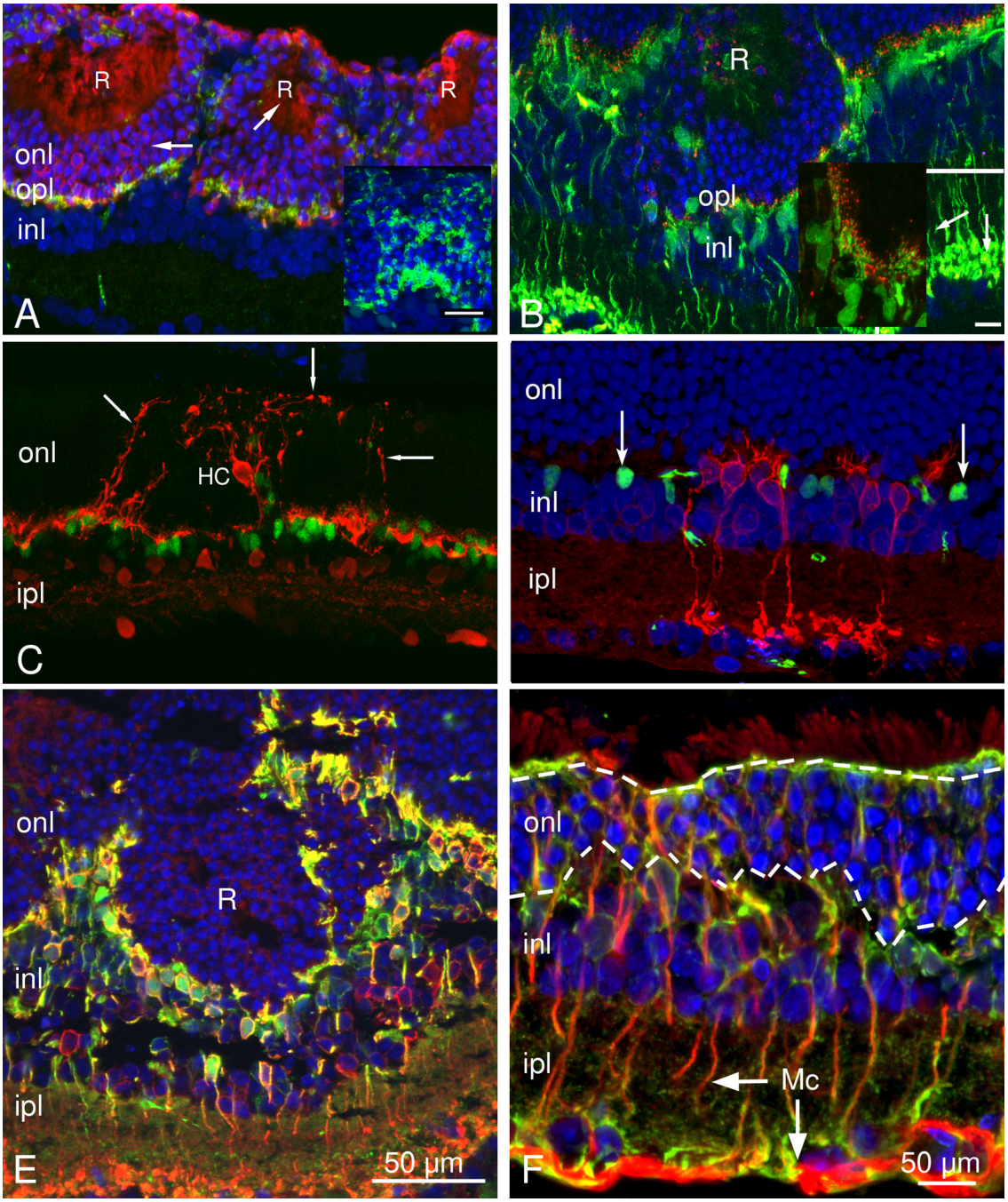

Figure 9.

Progressive retinal remodeling and degeneration in P16-P120 CKO retinas.

A: Retinal section from a P16 animal. A large rosette (R) was penetrated by rod bipolar cells, labeled green by PKCα antibodies. These cells contained the normal complement of synaptic proteins, including the glutamate receptor mGluR6 (red). The inset shows at high magnification mGluR6 positive puncta decorating the dendritic tips of rod bipolar cells within a rosette. B: Retinal section from a P30 animal. Three adjacent rosettes (R) are revealed by antibodies against recoverin (red). Blue: nuclear counterstaining. PSD95, a marker of photoreceptor synaptic terminals (green) was mislocalized between the rosette,

indicating displacement of photoreceptor terminals to ectopic locations. Inset shows the detail of ectopic expression of PSD95 (green) throughout the width of the onl.
C: Concomitant with rosette formation, photoreceptors and second order neurons were displaced to the outer retina and visibly remodeled in P35 retinas. The highlighted horizontal cell (HC), labeled red by calbindin D, sprouted profusely toward the outer retina (arrows), while the cell body migrated from the inner to the outer nuclear layer. The green stain is anti-Cre and thus denotes cells that are null for the Dicer protein.
D: At late stages, photoreceptors and inner retinal layers degenerated. Only 3–5 rows of photoreceptor nuclei remained in the onl of this 5 month-old retina. Rod bipolar cells (RB), stained with PKCα (red), were scant and showed poorly preserved dendritic arborizations. These cells were Cre-negative. A few Cre-positive cells (labeled green by anti-Cre antibodies) persisted in the inl (arrows). E: In this large rosette from a P45 retina, retinal layering was profoundly altered. Both rod and cone bipolar cells (stained red by PKCα and green by alphaGo antibodies) were present in the rosette and were found at ectopic retinal locations. Double-labeled cells (yellow) are rod bipolars, labeled by both antibodies.
F: Glial activation accompanied retinal degeneration in 3 month old CKO retinas. In this image, Müller glial cells (Mc) were stained both by glutamine synthase (green) and GFAP antibodies (red). The latter demonstrates that glial activation was widespread. Note the decrement in the number of photoreceptor rows to 2–5 from the 12–14 of a normal retina. onl: outer nuclear layer; opl: outer plexiform layer; inl: inner nuclear layer.

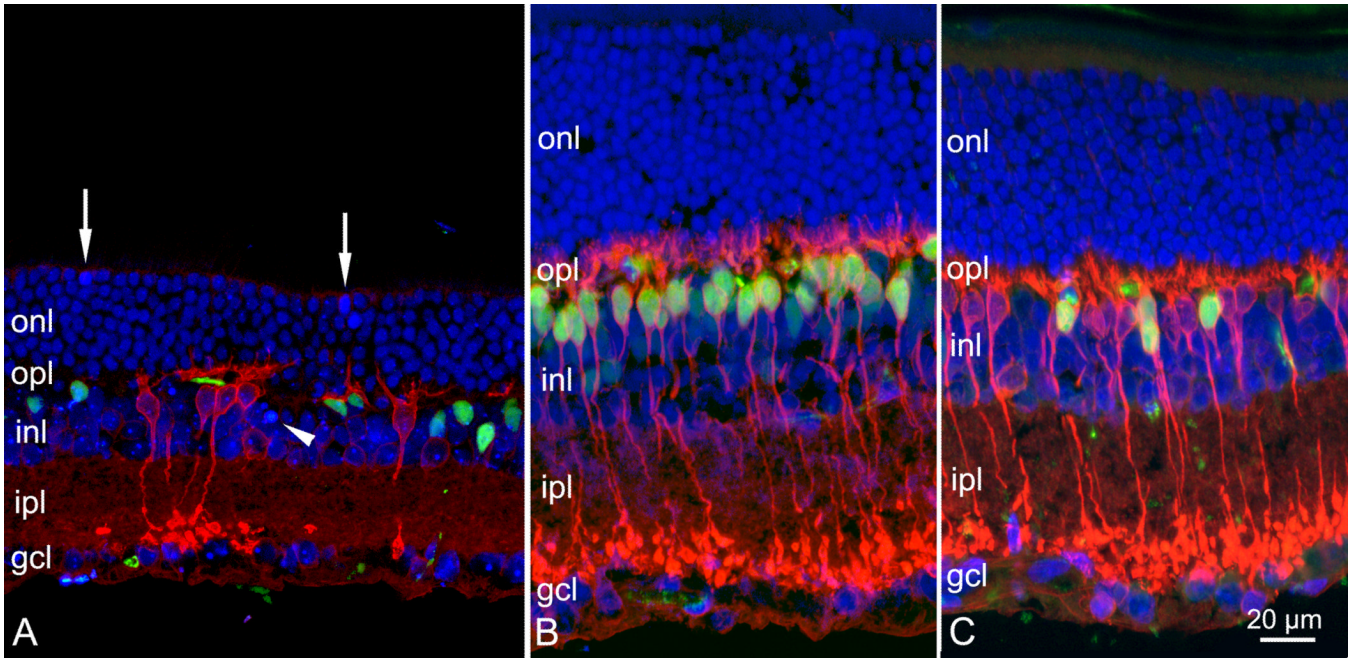

Figure 10.

Extensive degeneration of the CKO retina (A) at 5 months of age. Nuclei are stained blue by a fluorescent DNA binding molecule. Compared to an age-matched, wt retina (B), all the layers of the CKO appeared thinner. Rod bipolar cells, labeled red by PKCα antibody, were significantly reduced in number and displayed only rare and disorganized dendrites in comparison to their counterpart in the wt retina (B). Surviving rod bipolar cells in the CKO were largely Cre-negative while the number of Cre-positive cells (green labeling) was much decreased compared to the wt retina. Pycnotic nuclei, indicative of apoptotis, were visible in the onl (arrows) and in the inl (arrowhead) of the CKO retina. C: retinal section from a heterozygous animal, stained as the preparations shown in A and B. No evident alterations of the morphology were detectable in heterozygous individuals. onl: outer nuclear layer; opl: outer plexiform layer; inl: inner nuclear layer; ipl: inner plexiform layer; gcl: ganglion cell layer.

Table 1

Significance values for the ERG amplitudes shown in Fig. 2.

Scotopic a-wave	Scotopic b-wave	Photopic b-wave
WT vs. 1M −/−, p<0.001	WT vs. 1M −/−, p<0.001	WT vs. 1M −/−, p<0.001
WT vs. 1M +/−, NS	WT vs. 1M +/−, p<0.005	WT vs. 1M +/−, p<0.005
1M −/− vs. 1M +/−, NS	1M −/− vs. 1M +/−, p<005	1M −/− vs. 1M +/−, p<0.05
WT vs. 3M −/−, p<0.001	WT vs. 3M −/−, p<0.001	WT vs. 3M −/−, p<0.001
WT vs. 3M +/−, p<0.05	WT vs. 3M +/−, p<0.001	WT vs. 3M +/−, p<0 005
3M −/− vs. 3M +/−, p<0001	3M −/− vs. 3M +/−, p<0.001	3M −/− vs. 3M +/−, p<0.001
WT vs. 5M −/−, p<0.005	WT vs. 5M −/−, p<0.001	WT vs. 5M −/−, p<0.001
WT vs. 5M +/−, p<0.05	WT vs. 5M +/−, p<0.001	WT vs. 5M +/−, p<0.005
5M −/− vs. 5M +/−, p<0.01	5M −/− vs. 5M +/−, p<0.01	5M −/− vs. 5M +/−, NS